

Theoretical study of the mechanism of thermal decomposition of carbonate esters in the gas phase[†]

Rafael Notario,^{1*} Jairo Quijano,² Claudia Sánchez³ and Ederley Vélez²

¹Instituto de Química Física 'Rocasolano', CSIC, Serrano 119, 28006 Madrid, Spain

²Laboratorio de Físicoquímica Orgánica, Facultad de Ciencias, Universidad Nacional de Colombia, Sede Medellín, Apartado Aéreo 3840, Medellín, Colombia

³Politécnico Colombiano Jaime Isaza Cadavid, Apartado Aéreo, Medellín, Colombia

Received 3 November 2003; revised 26 December 2003; accepted 31 December 2003

ABSTRACT: Theoretical studies on the thermolysis in the gas phase of ethyl methyl and diethyl carbonates were carried out using *ab initio* theoretical methods at the MP2/6–31G(d) and MP2/6–311++G(2d,p) levels of theory. Two possible pathways were studied, one of them via a six-membered cyclic transition state and the other one in two steps, via a six- and a four-membered cyclic transition state, respectively, with the formation of an alcohol, ethylene and carbon dioxide. The nucleophilic substitution to give ethers was also studied. The results indicate that the reactions occur via a mechanism in two steps. The progress of the reactions was followed by means of the Wiberg bond indices. The kinetic parameters calculated for the studied reactions agree well with the available experimental results. Copyright © 2004 John Wiley & Sons, Ltd.

KEYWORDS: carbonate esters; decomposition; gas phase; mechanism; *ab initio*

INTRODUCTION

The thermal decompositions of carbonate esters have been experimentally investigated a number of times.^{1–14} They belong to that class of reactions known as pyrolytic *cis* eliminations,¹⁵ a class which includes the thermal decomposition of such compounds as esters, xanthates, amine oxides and organic halides. Carbonate pyrolysis is a *cis*-concerted elimination⁸ which takes place more rapidly than the reaction of the corresponding acetates.^{5,6} In general, it seems that esters lacking a β -hydrogen and therefore, unable to eliminate from the alkyl group, form the ether and carbon dioxide, whereas those that can do so decompose to the alcohol, olefin and carbon dioxide.

Much work has been done to establish the decomposition mechanism of the carbonates.^{2,3,10–13} Two mechanisms have been proposed to explain the thermolysis of carbonates with a β -hydrogen, that differ in the assignment of the oxygen atom, which is considered to play the

role of the nucleophilic agent in the hydrogen abstraction (see Fig. 1). In mechanism A, this role is assigned to the ether oxygen atom and pictures the reaction as a one-step process proceeding through a six-membered cyclic transition state. The other possibility, mechanism B, is that the carbonyl oxygen plays the role of hydrogen abstractor. This option also provides for the formation of a six-membered cyclic transition state whose decomposition, however, does not lead directly to all the observed products, but the initial alkoxy acid formed rapidly decomposes to give the alcohol and carbon dioxide. This two-step mechanism is similar to that proposed for ester pyrolysis. For carbonates and acetates, the C _{α} —O bond is fairly polar and breaking of this is the principal rate-determining step.¹³

Classical methods, such as steric and kinetic studies, have led to a general formulation of the reaction mechanism, but they afford no obvious method differentiating between the two mechanisms. Some decades ago, there was no firm evidence to implicate either of these mechanisms. Smith and co-workers^{1,2} favoured (A) on the basis of linear free energy arguments, but Cross *et al.*⁹ speculated that (B) is involved. Al-Awadi and Bigley¹¹ tried a direct and elegant approach to make the choice between mechanisms (A) and (B), labeling isotopically the various oxygen atoms of the carbonate and measuring the kinetic isotope effects. They tried this method for methyl *n*-hexyl carbonate but found the results vitiated by isotopic scrambling. In the case of xanthate pyrolysis (Chugaev reaction), in which both stepwise and concerted mechanisms of elimination exactly analogous to the carbonate

*Correspondence to: R. Notario, Instituto de Química Física 'Rocasolano', CSIC, Serrano 119, 28006 Madrid, Spain.

E-mail: rnotario@iqfr.csic.es

[†]Selected article presented at the Seventh Latin American Conference on Physical Organic Chemistry (CLAFQO-7), 21–26 September 2003, Florianópolis, Brazil.

Contact/grant sponsor: DIME, Dirección de Investigaciones Medellín, Universidad Nacional de Colombia, Sede Medellín; Contact/grant number: 030802675.

Contact/grant sponsor: COLCIENCIAS; Contact/grant number: 1118-05-11481.

Contact/grant sponsor: Dirección General de Investigación, Ministerio de Ciencia y Tecnología; Contact/grant number: BQU2000-1499.

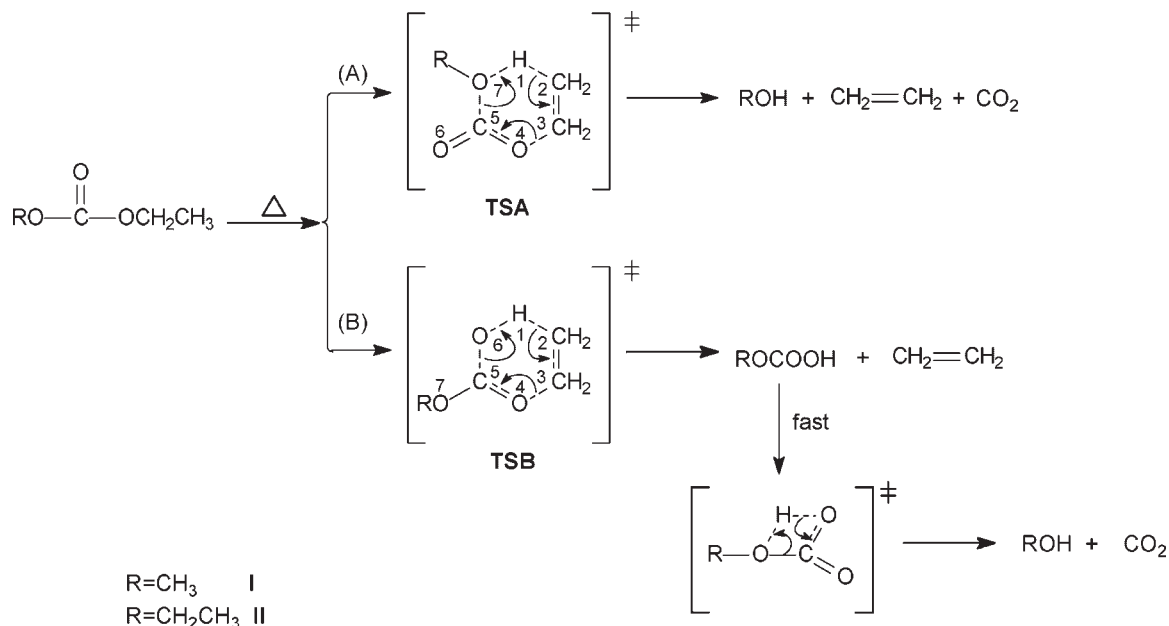


Figure 1. The two possible pathways in the thermolysis of carbonate esters

mechanisms (A) and (B) are possible, it has been unequivocally shown¹⁶ by such a kinetic isotope effect study that the elimination proceeds via a type (B) mechanism.

Another approach to the problem is to measure the kinetic effect of the introduction of chemical labels. Al-Awadi and Bigley^{11,12} used sulfur as a suitable chemical label.

It is now generally accepted that for carbonates containing a β -hydrogen, the only important initial process is a six-center retro-ene reaction followed by rapid decomposition of the alkoxy acid [mechanism (B) in Fig. 1].

In addition to the primary elimination for carbonate esters, a secondary reaction can occur. This is the nucleophilic substitution to give ethers, via a four-membered cyclic transition state, as depicted in Fig. 2.

To our knowledge, there have been no theoretical studies on these reactions at DFT or *ab initio* levels; there are only three studies, all of them at the AM1 semiempirical level. Lee *et al.*¹⁷ studied the pyrolysis in the gas phase of ethyl methyl and isopropyl methyl carbonate esters and Li *et al.*¹⁸ studied the thermal eliminations of carbonic acid and some of its esters. Kim *et al.*¹⁹ studied the substituent effects on thermal eliminations of aryl ethyl carbonates. Lee *et al.*¹⁷ concluded that the second

step in mechanism (B) is the rate-determining step and that the one-step mechanism (A) cannot be entirely ruled out. These conclusions disagree with the previous ideas but they are not safe owing to the low level of the calculations.

These facts prompted us to carry out a theoretical study of the mechanism of thermal decomposition of two carbonate esters: ethyl methyl carbonate, $\text{CH}_3\text{CH}_2\text{OC}(\text{O})\text{OCH}_3$ (**I**) and diethyl carbonate, $\text{CH}_3\text{CH}_2\text{OC}(\text{O})\text{OCH}_2\text{CH}_3$ (**II**). We studied the two possible mechanisms of the elimination, (A) and (B) (Fig. 1), and also the nucleophilic substitution to give ethers (Fig. 2).

Several experimental studies on the thermal decomposition of these species have been carried out.^{3,5,9,13,14} The experimental rate constants and the Arrhenius parameters obtained are collected in Table 1. The rate constants obtained in Ref. 3 are about a factor of 5–10 higher. All the other experimental rate constants are in fairly good agreement.

Table 1. Experimental Arrhenius parameters and rate constants for the thermal decomposition of ethyl methyl and diethyl carbonates

Compound	Log A	E_a (kJ mol ⁻¹)	$10^4 k$ (s ⁻¹) ^a	Ref.
Ethyl methyl carbonate, I	13.7	192.5	8.7	3
	11.72	182.0	0.75	9
	12.20	187.45	0.76	13
Diethyl carbonate, II	13.9	192.5	14.0	3
	13.2	194.1	2.0	5
	13.06	195.0	1.2	9
	13.03	193.6	1.5	13

^a At 600 K.

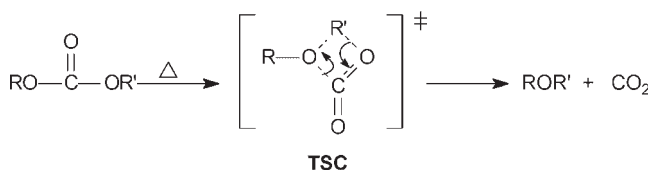


Figure 2. Mechanism of the nucleophilic substitution reaction to give ethers

All the experiments agree that equal amounts of ethylene, methanol (or ethanol) and carbon dioxide are formed. No ether was found. Both compounds decompose much faster than ethyl acetate, which indicates that the substitution of the methyl group by an additional methoxy or ethoxy group destabilizes the molecule by an appreciable factor.

COMPUTATIONAL DETAILS

All calculations were carried out using the Gaussian 98 computational package.²⁰ The geometric parameters for all the reactants, the transition states (TS) and the products of the reactions studied were fully optimized using *ab initio* analytical gradients at the MP2 level²¹ with the 6–31G(d) basis set.²² Each stationary structure was characterized as a minimum or a saddle point of first order by analytical frequency calculations. A scaling factor²³ of 0.9670 for the zero-point vibrational energies was used. Thermal corrections to enthalpy and entropy values were evaluated at the experimental temperature of 600.15 K. To calculate enthalpy and entropy values at a temperature T , the difference between the values at that temperature and 0 K was evaluated according to standard thermodynamics.²⁴

Transition vectors,²⁵ the eigenvectors associated with the unique negative eigenvalue of the force constant matrix, were obtained for all the transition states. Intrinsic reaction coordinate (IRC) calculations²⁶ were performed in all cases to verify that the localized transition-state structures connect with the corresponding minimum stationary points associated with reactants and products. All the optimized structures were fully reoptimized at the MP2/6–311++G(2d,p) level.²⁷

The bonding characteristics of the different reactants, transition states and products were investigated using a population partition technique, the natural bond orbital (NBO) analysis of Reed and co-workers.^{28,29} The NBO formalism provides values for the atomic natural total charges and also provides the Wiberg bond indices³⁰ used to follow the progress of the reactions. The NBO analysis was performed using the NBO program,³¹ implemented in the Gaussian 98 package,²⁰ and was carried out on the MP2 charge densities in order to include explicitly electron correlation effects.

We selected the classical transition-state theory (TST)^{32,33} to calculate the kinetic parameters. The rate constant, $k(T)$, for each elementary step of the kinetic scheme was computed using this theory assuming that the transmission coefficient is equal to unity, as expressed by the following relation:

$$k(T) = \frac{k_B T}{h} e^{\frac{-\Delta G^\ddagger(T)}{RT}} \quad (1)$$

where k_B , h and R are the Boltzmann constant, Planck's constant and the universal gas constant, respectively, and

$\Delta G^\ddagger(T)$ is the standard-state free energy of activation at the absolute temperature T .

The activation energies, E_a , and the Arrhenius A factors were calculated using Eqns (2) and (3), respectively, derived from the TST ($e = 2.718$):

$$E_a = \Delta H^\ddagger(T) + RT \quad (2)$$

$$A = \frac{ek_B T}{h} e^{\frac{\Delta S^\ddagger(T)}{R}} \quad (3)$$

RESULTS AND DISCUSSION

Theoretical calculations at the MP2/6–311++G(2d,p) level of theory were carried out in order to explore the nature of the reaction mechanism for the unimolecular decomposition of ethyl methyl and diethyl carbonates in the gas phase. We investigated two pathways, as shown in Fig. 1: a one-step process proceeding through a six-membered cyclic transition state, in which the ether oxygen atom participates, and a two-step process, with an initial rate-determining step via a six-membered cyclic transition state in which the carbonyl oxygen atom participates, followed by rapid decomposition of the alkoxy acid formed. In both mechanisms the final products are the same: ethylene, carbon dioxide and an alcohol.

We also investigated a secondary reaction that can occur in the thermolysis of carbonate esters, namely nucleophilic substitution to give ethers (see Fig. 2).

Electronic energies, zero-point vibrational energies, thermal correction to enthalpies and entropies for all the reactants, transition states and products involved in all of the steps of the two reactions studied are given in Table 2.

Free energy profiles for the decomposition processes of the two carbonate esters studied are presented in Figs 3 and 4.

The calculated activation free energies for the first step of the process following mechanism (B) are 192.8 and 193.3 kJ mol^{−1} for reactions I and II, respectively, and the calculated activation free energies of the second step are 155.4 and 136.9 kJ mol^{−1}, respectively.

The overall processes are highly exergonic, with reaction free energies of −135.0 and −136.9 kJ mol^{−1} for reactions I and II, respectively.

As can be observed in Figs 3 and 4, the activation free energies of the processes following the mechanism (A) are higher than those corresponding to the first step of mechanism (B). They are 241.3 and 238.4 kJ mol^{−1} for reactions I and II, respectively, 48.5 and 45.1 kJ mol^{−1} higher than the corresponding values for mechanism (B). This result confirms the idea derived from experiments that in the thermolysis of carbonates containing a

Table 2. Electronic energies evaluated at the MP2/6–311++G(2d,p)//MP2/6–31G(d) level, zero-point vibrational energies, *ZPE*, and Thermal Corrections to Enthalpies, *TCH*, in hartree and entropies, *S*, in cal mol^{−1} K^{−1} for all the reactants, transition states and products involved in the thermal decomposition of ethyl methyl (I) and diethyl (II) carbonates

Species	MP2/6–311++G(2d,p)//MP2/6–31G(d)	<i>ZPE</i> ^a	<i>TCH</i> ^{a,b}	<i>S</i> ^{a,b}
I	−382.103083	0.127415	0.154670	112.956
TSA-I	−382.001753	0.118572	0.146477	114.553
TSB-I	−382.020734	0.119935	0.147148	114.651
TSC-I	−381.989469	0.122898	0.150531	115.056
TSB2-I	−303.644225	0.062727	0.080434	89.748
CH ₃ COOH	−303.710178	0.068976	0.086891	89.216
CH ₂ =CH ₂	−78.361795	0.052038	0.062441	61.388
CH ₃ OH	−115.469332	0.052597	0.063267	65.822
CO ₂	−188.245426	0.011510	0.020065	58.329
CH ₃ CH ₂ OCH ₃	−193.864064	0.111477	0.130719	89.805
II	−421.310201	0.156825	0.188562	123.807
TSA-II	−421.209087	0.147874	0.180344	126.310
TSB-II	−421.227562	0.149319	0.181042	125.635
TSC-II	−421.198050	0.152360	0.184441	125.534
TSB2-II	−342.852667	0.092104	0.114288	101.025
CH ₃ CH ₂ COOH	−342.911647	0.098201	0.120638	100.291
CH ₃ CH ₂ OH	−154.676036	0.082189	0.097133	77.852
(CH ₃ CH ₂) ₂ O	−233.071556	0.140703	0.164609	102.128

^a Evaluated at the MP2/6–31G(d) level.

^b Evaluated at 600.15 K.

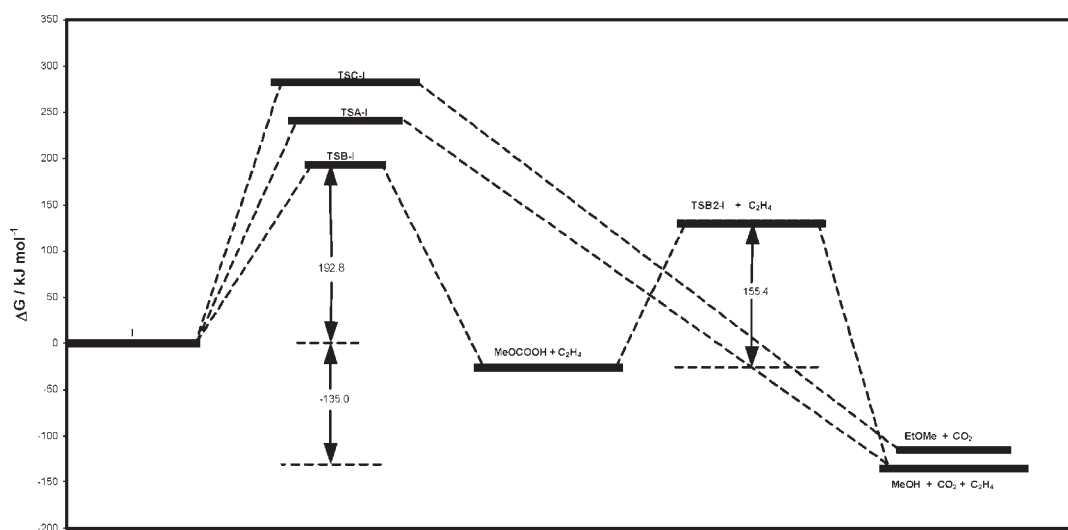


Figure 3. Free energy profile at 600.15 K, evaluated at the MP2/6–311++G(2d,p)//MP2/6–31G(d) level, for the decomposition process of ethyl methyl carbonate ester. Relative free energy values (with respect to reactant I, in kJ mol^{−1}) of the stationary points found are as follows: **TSA-I**, 241.3; **TSB-I**, 192.8; **TSC-I**, 282.5; MeOCOOH + C₂H₄, −26.3; **TSB2-I** + C₂H₄, 129.1; EtOMe + CO₂, −115.0; MeOH + CO₂ + C₂H₄, −135.0

β -hydrogen the only important initial process is a six-center retro-ene reaction followed by the decomposition of the alkoxy acid formed, mechanism (B) in Fig. 1.

We carried out a detailed study of the two steps of this mechanism. The first step is the rate-limiting step. There is one and only one imaginary vibrational frequency in the transition states for this first step of the studied thermal decomposition reactions (1629.8i and 1627.9i cm^{−1} for **TSB-I** and **TSB-II**, respectively, evaluated at the MP2/6–31G(d) level of theory, with the

lowest real frequency being 18.2 and 16.6 cm^{−1} for **TSB-I** and **TSB-II**, respectively). The optimized structures for these transition states are shown in Fig. 5.

During the thermolysis process, when the reactant is being transformed into its transition state, the H-1—C-2, C-3—O-4 and C-5—O-6 distances are increasing, whereas the C-2—C-3, O-4—C-5 and O-6—H-1 distances are decreasing. The distances in both transition states are practically identical, indicating that the alkoxy group attached to C-5 does not influence either the

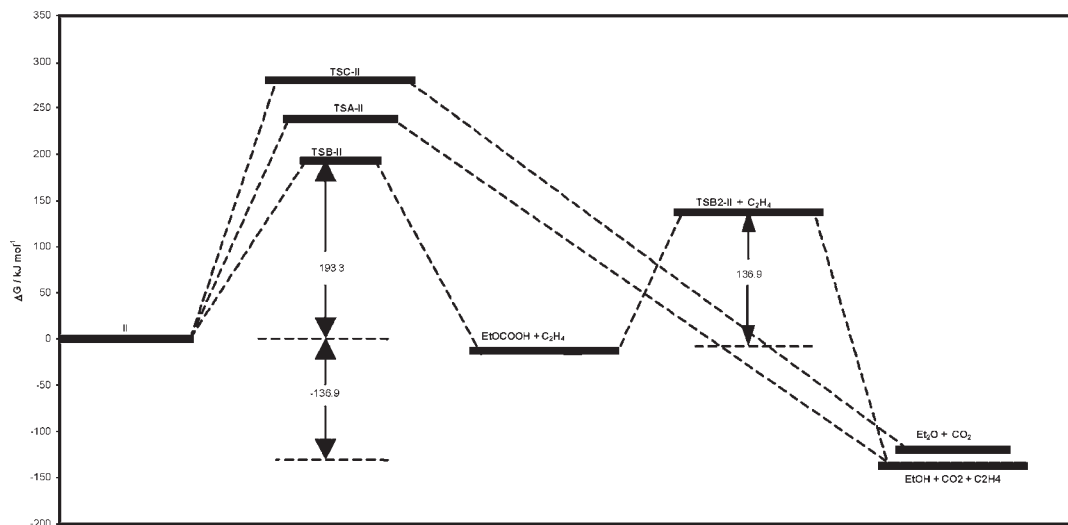


Figure 4. Free energy profile at 600.15 K, evaluated at the MP2/6–311++G(2d,p)//MP2/6–31G(d) level, for the decomposition process of diethyl carbonate ester. Relative free energy values (with respect to reactant **II**, in kJ mol^{-1}) of the stationary points found are as follows: **TSA-II**, 238.4; **TSB-II**, 193.3; **TSC-II**, 280.0; $\text{EtOCCOOH} + \text{C}_2\text{H}_4$, -12.4; **TSB2-II** + C_2H_4 , 124.5; $\text{Et}_2\text{O} + \text{CO}_2$, -119.6; $\text{EtOH} + \text{CO}_2 + \text{C}_2\text{H}_4$, -136.9

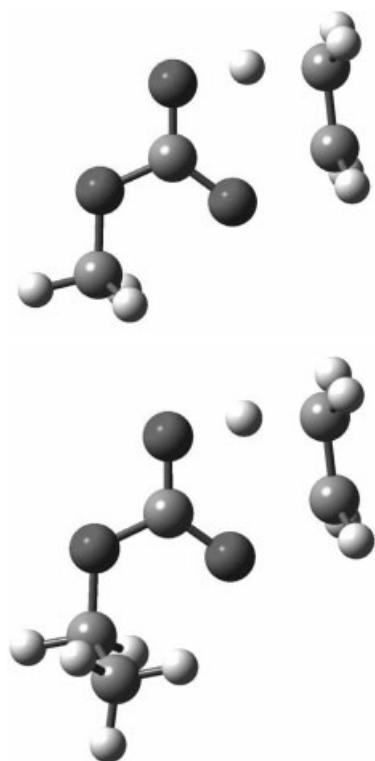


Figure 5. Structures of the transition states, **TSB-I** and **TSB-II**, corresponding to the first step of mechanism (B) in the thermolysis of ethyl methyl and diethyl carbonate esters, optimized at the MP2/6–31G(d) level of theory

hydrogen migration from C-2 to O-6 or the O-4—C-5 double-bond formation. The main distances in reactants and transition states are shown in Table 3.

The transition vectors, TV, associated with the unique negative eigenvalue of the Hessian matrix for the transi-

tion states of the studied reactions are shown in Table 4. The main components of the TV are the H-1—C-2 and O-6—H-1 distances and the C-2—H-1—O-6 and C-5—O-6—H-1 bond angles. The largest component (around 19–22%) of TV corresponds to the two distances associated to the hydrogen migration process from C-2 to O-6.

As in other theoretical studies on reaction mechanisms carried out by us,^{34–36} the progress of the reactions has been followed by means of the Wiberg bond indices,³⁰ B_i , to avoid the subjective aspects associated with geometric analysis of the transition states. A very precise image of the timing and extent of the bond-breaking and bond-forming processes along the reaction path can be achieved³⁷ by analyzing the evolution of the bond indices corresponding to the bonds being broken or made in a chemical reaction.

The Wiberg bond indices corresponding to the bonds involved in the reaction center of the first step of the two reactions studied, for all the reactants, transition states and products, are given in Table 5.

Moyano *et al.*³⁷ defined a relative variation of the bond index at the transition state, δB_i , for every bond, i , involved in a chemical reaction as

$$\delta B_i = \frac{(B_i^{\text{TS}} - B_i^{\text{R}})}{(B_i^{\text{P}} - B_i^{\text{R}})} \quad (4)$$

where the superscripts R, TS and P refer to reactants, transition states and products, respectively. Hence it is possible to calculate the percentage evolution (%EV) of the bond order through the chemical step by means of³⁸

$$\%EV = 100\delta B_i \quad (5)$$

Table 3. Main distances (Å) in reactants and transition states of the first step of mechanism (B), optimized at the MP2/6–31G(d) Level

Species	H-1—C-2	C-2—C-3	C-3—O-4	O-4—C-5	C-5—O-6	O-6—H-1
I	1.092	1.514	1.451	1.344	1.219	2.688
TSB-I	1.335	1.398	1.957	1.271	1.274	1.286
II	1.091	1.514	1.451	1.345	1.220	2.684
TSB-II	1.335	1.399	1.955	1.273	1.274	1.286

Table 4. Hessian unique negative eigenvalues and main components of the transition vectors for the transition states of the first step of the studied reactions, calculated at the MP2/6–31G(d) level (all values in au)

	TSB-I	TSB-II
Eigenvalue	−0.37994	−0.29367
H-1—C-2	0.455	0.462
C-2—C-3	−0.289	−0.273
O-4—C-5	−0.186	−0.172
C-5—O-6	0.180	0.156
O-6—H-1	−0.435	−0.474
C-2—H-1—O-6	0.374	0.418
C-5—O-6—H-1	0.313	0.242
O-6—C-5—O-7	−0.192	−0.170
O-4—C-5—O-7	0.123	0.126
H-1—C-2—C-3—H	0.112	0.131
H-1—C-2—C-3—H'	−0.133	−0.135
H—C-2—C-3—H	0.180	0.197
H—C-2—C-3—H'	−0.196	−0.199

The calculated percentages of evolution of the bonds involved in the reaction center are given in Table 5. As can be seen, the breaking of the C-3—O-4 bond is the more advanced process (63%). The H-1—C-2 bonds are broken to the extent of 52% whereas the O-6—H-1 bonds are only 38–39% formed.

The average value, δB_{av} , calculated as³⁷

$$\delta B_{av} = \frac{1}{n} \sum \delta B_i \quad (6)$$

where n is the number of bonds involved in the reaction, measures the degree of advancement of the transition state along the reaction path. Calculated δB_{av} values for the first step of the studied reactions are given in Table 5. As can be seen, the δB_{av} values show that the transition states have an 'early' character, nearer to the reactants than to the products.

The synchronicity, S_y , of a chemical reaction can be calculated as

$$S_y = 1 - A \quad (7)$$

where A is the asynchronicity, calculated using the expression proposed by Moyano *et al.*:³⁷

$$A = \frac{1}{(2N - 2)} \sum \frac{|\delta B_i - \delta B_{av}|}{\delta B_{av}} \quad (8)$$

Synchronicities vary between zero and one, which is the case when all of the bonds implicated in the reaction center have broken or formed at exactly the same extent in the TS. The S_y values obtained in this way are, in principle, independent of the degree of advancement of the transition state. The S_y values calculated for the reactions studied are shown in Table 5. The synchronicities are 0.90 in both cases, indicating that the mechanisms correspond to slightly asynchronous processes.

Another aspect to be taken into account is the relative asynchronicity of the bond-breaking and the bond-forming processes that measures the 'bond deficiency' along

Table 5. Wiberg bond indices, B_i , of reactants, transition states and products of the studied reactions, percentage evolution, %EV, through the chemical process of the bond indices at the transition states, degree of advancement of the transition states, δB_{av} , and absolute synchronicities, S_y [values calculated at the MP2/6–31G(d) level]

		H-1—C-2	C-2—C-3	C-3—O-4	O-4—C-5	C-5—O-6	O-6—H-1
Reaction I	B_i^R	0.930	1.030	0.830	1.001	1.640	0.001
	B_i^{TS}	0.445	1.351	0.309	1.316	1.317	0.271
	B_i^P	0.000	2.034	0.000	1.654	1.000	0.711
	%EV	52.2	32.0	62.8	48.2	50.5	38.0
				$\delta B_{av} = 0.473$; $S_y = 0.896$			
Reaction II	B_i^R	0.929	1.030	0.831	1.000	1.631	0.001
	B_i^{TS}	0.445	1.350	0.310	1.308	1.317	0.271
	B_i^P	0.000	2.034	0.000	1.682	0.966	0.699
	%EV	52.1	31.9	62.7	45.2	47.2	38.9
				$\delta B_{av} = 0.463$; $S_y = 0.901$			

Table 6. NBO charges, calculated at the MP2/6–31G(d) level, at the atoms involved in the reactions

Species	H-1	C-2	C-3	O-4	C-5	O-6
<i>First step of the pathway</i>						
I	0.235	−0.674	−0.004	−0.647	1.263	−0.766
TSB-I	0.470	−0.884	0.042	−0.810	1.293	−0.811
II	0.235	−0.674	−0.044	−0.647	1.261	−0.760
TSB-II	0.477	−0.883	0.036	−0.782	1.292	−0.843

Table 7. Calculated^{a,b} kinetic and activation parameters for the studied reactions

Reaction	$10^4 k$ (s ^{−1})	E_a (kJ mol ^{−1})	Log A	ΔH^\ddagger (kJ mol ^{−1})	ΔG^\ddagger (kJ mol ^{−1})	ΔS^\ddagger (J mol ^{−1} K ^{−1})
I	2.08	202.1	13.9	197.1	192.8	7.1
II	1.88	202.9	13.9	197.9	193.3	7.6

^a Values calculated at the MP2/6–311++G(2d,p)//MP2/6–31G(d) level of theory.^b At 600.15 K.

the reaction path. In the studied reactions, the bond-breaking processes are more advanced (54–55%) than the bond-forming processes (39%), indicating a bond deficiency in the transition states.

The charge distribution in reactants and transition states was analyzed by means of the NBO analysis of Weinhold and co-workers^{28,29} In Table 6, the natural atomic charges at the atoms involved in the reaction center are given. There is an important positive charge developed on H-1 (0.24 at reactants and 0.47–0.48 at TSs), whereas the electronic excess is supported by C-2 (−0.67 at reactants and −0.88 at TSs) and by the two oxygens [−0.65 at reactants and −(0.78–0.81) at TSs for O-4 and −(0.76–0.77) at reactants and −(0.81–0.84) at TSs for O-6]. The negative character of O-6 allows it to attract the H-1 in the TS.

The kinetic parameters for the two reactions studied here were calculated at the MP2/6–311++G(2d,p)//MP2/6–31G(d) level at the same temperature as used in the experiments, 600.15 K. These data are given in Table 7 and can be compared with the experimental results in Table 1. The calculated rate constants agree very well with the experimentally determined values in the case of diethyl carbonate, whereas in the case of ethyl methyl carbonate the calculated rate constant is about three times higher.

The nature of the non-reacting alkoxy group seems to have little effect on the rate constant. The calculated values are very close for both reactions.

In the second step of the pathway, the alkoxy acid intermediate initially formed decomposes to CO₂ and the corresponding alcohol. The TSs of this step have a four-membered cyclic structure. They present one and only one imaginary vibrational frequency, 1709.3i and 1707.4i cm^{−1} for TSB2-I and TSB2-II, respectively, with the lowest real frequency being 136.5 and 77.3 cm^{−1}, respectively.

This second step of mechanism (B) is a more rapid process than the first step, with activation free energies of 155.4 and 136.9 kJ mol^{−1} for reactions I and II, respectively, and so it is not the rate-limiting step of the reactions. The calculated rate constants of the decomposition of the alkoxy acids to methanol (or ethanol) and carbon dioxide are 0.37 and 15.2 s^{−1} for reactions I and II, respectively, evaluated at the MP2/6–311++G(2d,p)//MP2/6–31G(d) level of theory.

As can be observed in Figs 3 and 4, the nucleophilic substitution to give ethers, via the four-membered cyclic transition states **TSC-I** and **TSC-II**, presents high free energies of activation, 282.5 and 280.0 kJ mol^{−1}, respectively, these TSs being 89.7 and 86.7 kJ mol^{−1} higher than **TSB-I** and **TSB-II**, respectively. This result indicates that the nucleophilic substitution to give ethers is not a competitive process against elimination. This is accord with the experimental fact that no ethers were found in the experiments.

CONCLUSIONS

A theoretical study on the thermolysis of two carbonate esters, ethyl methyl and diethyl carbonate, was carried out at the MP2/6–31G(d) and MP2/6–311++G(2d,p) levels of theory.

The results indicate that the mechanism is a two-step process. The first step, which is rate determining, occurs via a six-membered cyclic transition state in which the carbonyl oxygen participates, followed by a rapid decomposition of the alkoxy acid formed via a four-membered cyclic transition state. The other mechanism proposed, in one step, presents higher free energies of activation.

The transition states present an ‘early’ character, nearer to the reactants than to the products. The breaking of the

C $_{\alpha}$ —O bond is the more advanced process. The processes are slightly asynchronous.

The calculated rate constants agree well with the available experimental values. The nature of the non-reacting alkoxy group seems to have little effect on the rate constant.

Acknowledgments

This work was supported by a research fund provided by DIME, Dirección de Investigaciones Medellín, Universidad Nacional de Colombia, Sede Medellín (Project No. 030802675), and COLCIENCIAS (Project No. 1118-05-11481), and by the Spanish Dirección General de Investigación, Ministerio de Ciencia y Tecnología (Project No. BQU2000-1499).

REFERENCES

- Smith GG, Kösters B. *Chem. Ber.* 1960; **93**: 2400–2404.
- Smith GG, Jones DAK, Taylor R. *J. Org. Chem.* 1963; **28**: 3547–3550.
- Gordon AS, Norris WP. *J. Phys. Chem.* 1965; **69**: 3013–3017.
- Smith GG, Lum KK, Kirby JA, Posposil J. *J. Org. Chem.* 1969; **34**: 2090–2095.
- Bigley DB, Wren CM. *J. Chem. Soc., Perkin Trans. 2* 1972; 926–928.
- Bigley DB, Wren CM. *J. Chem. Soc., Perkin Trans. 2* 1972; 1744–1745.
- Bigley DB, Wren CM. *J. Chem. Soc., Perkin Trans. 2* 1972; 2359–2361.
- Bigley DB, Brown C, Weatherhead RH. *J. Chem. Soc., Perkin Trans. 2* 1976; 701–703.
- Cross JTD, Hunter R, Stimson VR. *Aust. J. Chem.* 1976; **29**: 1477–1481.
- Amin HB, Taylor R. *J. Chem. Soc., Perkin Trans. 2* 1978; 1090–1095.
- Al-Awadi N, Bigley DB. *J. Chem. Soc., Perkin Trans. 2* 1979; 497–500.
- Al-Awadi N, Bigley DB. *J. Chem. Soc., Perkin Trans. 2* 1982; 773–775.
- Taylor R. *J. Chem. Soc., Perkin Trans. 2* 1983; 291–296.
- Herzler J, Manion JA, Tsang W. *J. Phys. Chem. A* 1997; **101**: 5494–5499.
- DePuy CH, King RW. *Chem. Rev.* 1960; **60**: 431–457.
- Bader RFW, Bourns AN. *Can. J. Chem.* 1961; **39**: 348–358.
- Lee I, Cha OJ, Lee BS. *Bull. Korean Chem. Soc.* 1991; **12**: 97–101.
- Li Y, Hong S, Wang S. *Wuli Huaxue Xuebao* 1995; **11**: 414–418; *Chem. Abstr.* 1995; **123**: 111291.
- Kim CK, Lee BS, Lee I. *J. Phys. Org. Chem.* 1993; **6**: 215–222.
- Frisch MJ, Trucks GW, Schlegel HB, Scuseria GE, Robb MA, Cheeseman JR, Zakrzewski VG, Montgomery JA Jr, Stratmann RE, Burant JC, Dapprich S, Millam JM, Daniels AD, Kudin KN, Strain MC, Farkas O, Tomasi J, Barone V, Cossi M, Cammi R, Mennucci B, Pomelli C, Adamo C, Clifford S, Ochterski J, Petersson GA, Ayala PY, Cui Q, Morokuma K, Salvador P, Dannenberg JJ, Malick DK, Rabuck AD, Raghavachari K, Foresman JB, Cioslowski J, Ortiz JV, Baboul AG, Stefanov BB, Liu G, Liashenko A, Piskorz P, Komaromi I, Gomperts R, Martin RL, Fox DJ, Keith T, Al-Laham MA, Peng CY, Nanayakkara A, Challacombe M, Gill PMW, Johnson B, Chen W, Wong MW, Andrés JL, González C, Head-Gordon M, Replogle ES, Pople JA. *Gaussian 98, Revision A.11.3*. Gaussian: Pittsburgh, PA, 2001.
- Møller C, Plesset M. *Phys. Rev.* 1934; **46**: 618–622.
- Ditchfield R, Hehre WJ, Pople JA. *J. Chem. Phys.* 1971; **54**: 724–728.
- Scott PA, Radom L. *J. Phys. Chem.* 1996; **100**: 16502–16513.
- McQuarrie DA, Simon JD. *Molecular Thermodynamics*. University Science Books: Sausalito, CA, 1999.
- McIver JV Jr. *Acc. Chem. Res.* 1974; **7**: 72–77.
- Fukui K. *J. Phys. Chem.* 1970; **74**: 4161–4163.
- Clark T, Chandrasekhar J, Spitznagel GW, Schleyer PvR. *J. Comput. Chem.* 1983; **4**: 294–301.
- Reed AE, Weinhold F. *J. Chem. Phys.* 1983; **78**: 4066–4073.
- Reed AE, Curtiss LA, Weinhold F. *Chem. Rev.* 1988; **88**: 899–926.
- Wiberg KB. *Tetrahedron* 1968; **24**: 1083–1096.
- Glendening ED, Reed AE, Carpenter JE, Weinhold F. *NBO, Version 3.1*. Madison, WI, 1988.
- Glasstone KJ, Laidler KJ, Eyring H. *The Theory of Rate Processes*. McGraw-Hill: New York, 1941; Chapt. 4.
- Benson SW. *The Foundations of Chemical Kinetics*. McGraw-Hill: New York, 1969.
- Quijano J, Notario R, Chamorro E, León LA, Sánchez C, Alarcón G, Quijano JC, Chuchani G. *J. Phys. Org. Chem.* 2002; **15**: 413–419.
- Chamorro E, Quijano J, Notario R, Sánchez C, León LA, Chuchani G. *Int. J. Quantum Chem.* 2003; **91**: 618–625.
- Notario R, Quijano J, León LA, Sánchez C, Quijano JC, Alarcón G, Chamorro E, Chuchani G. *J. Phys. Org. Chem.* 2003; **16**: 166–174.
- Moyano A, Pericàs MA, Valentí E. *J. Org. Chem.* 1989; **54**: 573–582.
- Domingo LR, Picher MT, Safont VS, Andrés J, Chuchani G. *J. Phys. Chem. A* 1999; **103**: 3935–3943.